NACA RM L51G18

NACA

RESEARCH MEMORANDUM

FLIGHT INVESTIGATION AT SUBSONIC, TRANSONIC, AND SUPERSONIC VELOCITIES OF THE HINGE-MOMENT CHARACTERISTICS, LATERAL-CONTROL EFFECTIVENESS, AND WING DAMPING IN ROLL OF A 60° SWEPTBACK DELTA WING WITH HALF-DELTA TIP AILERONS

(Revised)

By C. William Martz and James D. Church

Langley Aeronautical Laboratory
Langley Field, Va.

NATIONAL ADVISORY COMMITTEE FOR AERONAUTICS

WASHINGTON
September 21, 1951

NATIONAL ADVISORY COMMITTEE FOR AERONAUTICS

RESEARCH MEMORANDUM

FLIGHT INVESTIGATION AT SUBSONIC, TRANSONIC, AND SUPERSONIC VELOCITIES OF THE HINGE-MOMENT CHARACTERISTICS, LATERAL-CONTROL EFFECTIVENESS, AND WING DAMPING IN ROLL OF A 60° SWEPTBACK DELTA WING WITH HALF-DELTA TIP AILERONS[1]

(Revised)

By C. William Martz and James D. Church

SUMMARY

A flight investigation of an NACA hinge-moment roll research model consisting of a sharp-nosed cylindrical body equipped with a cruciform arrangement of 60° sweptback delta wings, two of which were equipped with half-delta tip controls, was conducted at the Langley Pilotless Aircraft Research Station at Wallops Island, Va. Reduced data, obtained at zero angle of attack, are presented as the variation with Mach number of damping-in-roll coefficient, aileron rolling-moment coefficient, lateral-control effectiveness, and hinge-moment coefficient at various deflections.

Results indicated that the half-delta tip aileron (hinge line at 63.5 percent aileron root chord) was very well balanced, especially at transonic and supersonic speeds. Hinge-moment coefficients were found to reduce abruptly at a Mach number of 0.91, indicating a rapid rearward center-of-pressure shift.

The measured damping-in-roll coefficients were approximately 34 percent lower than the values predicted by linear theory at supersonic Mach numbers. Subsonic values of the damping-in-roll coefficient were found to be about 28 percent lower than predicted by lifting-line theory corrected for sweepback and compressibility effects.

Aileron rolling-moment coefficients were found to be approximately 78 percent of the values predicted by linear theory at supersonic Mach

---

[1]Originally issued Feb. 7, 1950 as NACA RM L9L14.

numbers. There were no abrupt changes in aileron rolling-moment coefficients at transonic speeds.

Rolling effectiveness of a delta-wing configuration, calculated from reduced data of the investigation, agreed favorably with previous rocket-test results. Only a small loss in rolling effectiveness was obtained at transonic speeds. The delta-wing configuration was found to retain more than half of its subsonic rolling effectiveness at a Mach number of 1.5.

INTRODUCTION

As part of an endeavor to provide aerodynamic design data for guided missiles and high-speed aircraft, a free-flight program was initiated to determine the hinge-moment and rolling characteristics of a series of promising wing-aileron configurations. It had been indicated from free-flight rocket tests (reference 1) that half-delta wing-tip ailerons provide satisfactory lateral-control effectiveness throughout the transonic and low-supersonic speed ranges. It was further realized that half-delta tip ailerons provided ample opportunity for aerodynamic balance, both because of the mechanical ease of locating hinge axes and because of the small movement of center of pressure with moderate changes in deflection angle and Mach number. In addition, it was known that thin, highly swept wings of low aspect ratio offer the advantage of low drag. Therefore, a 60° sweptback delta wing with half-delta tip ailerons was chosen as the first of this series for the present investigation.

Results obtained in this investigation included hinge moments, damping-in-roll moments, aileron rolling moments, and rolling effectiveness from Mach numbers of 0.69 to 1.52 for all aileron deflections between ±5° at zero angle of attack.

SYMBOLS

b	wing span, 2.58 feet
$\bar{c}$	wing mean aerodynamic chord, 1.49 feet
$\bar{c}_a$	aileron mean aerodynamic chord, 0.385 foot
S	total wing area in one plane, 2.89 square feet
S_a	area of one aileron, 0.095 square foot
δ	deflection of one aileron, degrees
$\dot{\varphi}$, p	rate of roll, radians per second

M Mach number

ρ mass density of air, slugs per cubic foot

V free-stream velocity, feet per second

q dynamic pressure, pounds per square foot $\left(\frac{\rho V^2}{2}\right)$

μ coefficient of viscosity of air, slugs per cubic foot-second

R Reynolds number $\left(\frac{\rho \bar{c} V}{\mu}\right)$

a_l longitudinal acceleration of model, g units

g acceleration of gravity

C_h aileron hinge-moment coefficient

$$\left(\frac{\text{Hinge moment about hinge line}}{qS_a\bar{c}_a}\right)$$

C_{l_p} damping-in-roll coefficient, per radian

$$\left(\frac{\text{Damping-in-roll moment on damping wings}}{\frac{pb}{2V}\,qbS}\right)$$

C_{l_δ} aileron rolling-moment coefficient, per degree

$$\left(\frac{\text{Total aileron rolling moment}}{\delta qbS}\right)$$

All rolling moments are taken about the longitudinal axis.

MODEL

The hinge-moment roll research model used in this investigation consisted of a sharp-nosed cylindrical body equipped with a cruciform arrangement of 60° sweptback delta wings. A drawing of the model and booster showing the over-all dimensions is presented in figure 1, and a photograph of the model is shown as figure 2.

Two of the diametrically opposite wings were equipped with tip ailerons and two of the wings were affixed to a rolling-moment balance beam as shown diagrammatically in figure 3. The wing panels had a modified hexagonal airfoil section, the maximum thickness ratio of which varied linearly from 2.32 percent at the root chord (at fuselage center line) to 9 percent at the parting line of the wing and aileron. The half-delta tip ailerons, fastened to the outboard ends of torque rods, had modified double-wedge airfoil sections with a constant thickness-to-chord ratio of 3 percent. The gap between the aileron and a fence mounted on the tip chord of the wing panel was 0.01 inch. Figure 4 is a sketch showing the detail dimensions of the wing and aileron, and figure 5 is a photograph of the wing-aileron assembly. The latter figure also illustrates the gap existing between the fuselage skin and the damping-wing surface.

It was found from preflight wing torsion tests that estimated flight loads would produce negligible wing twist.

INSTRUMENTATION

The model was equipped with an NACA telemeter which transmitted the following flight data: normal and longitudinal acceleration, static and total-head pressure, aileron deflection and hinge moment, angular rolling velocity, and rolling moment.

A balance to measure aileron hinge moments and a control-position indicator to measure aileron deflections were constructed as integral parts of a control power unit, the unit being mounted in the after part of the wing section.

Rolling moment was obtained by rigidly mounting the two damping-in-roll wings to the free end of a steel cantilever balance beam. No artificial damping was employed in this assembly.

In addition to this model instrumentation, a radiosonde recorded atmospheric data at all altitudes shortly after firing. Flight-path data were obtained with a radar tracking unit and CW Doppler radar was used to determine initial flight velocities. Photographic tracking was also employed to obtain a visual record of any flight peculiarities or structural failures during the flight.

TECHNIQUE

The technique utilized in this investigation consisted of mechanically pulsing the ailerons throughout the entire flight such that their deflection varied sinusoidally with time. The pulsing frequency was 4 cycles per second and the amplitude ±5°. This technique enabled hinge-moment data to be obtained for all aileron deflections over the complete Mach number range tested. All hinge-moment data were corrected for the inertia effects of the aileron and control linkage caused by the pulsing motion as well as the load-deflection effects of the control linkage.

The response of the model to the sinusoidal control input involved motion about the roll axis only (as was substantiated by a normal accelerometer reading of zero obtained throughout the flight). Thus, angle-of-attack effects were considered negligible upon the results. By considering the model to be restricted to one degree of freedom (roll), the aileron rolling moments were determined by an application of the method of least squares, as is shown in the appendix.

Wing rolling moments were measured directly by telemetered deflections of the rolling-moment balance beam from which the wing damping-in-roll was determined as shown in the appendix.

ACCURACY

Although hinge moments were measured directly from telemetered deflections of a calibrated hinge-moment beam, errors were introduced into these measurements largely by inaccuracies in instrumentation.

Instrument phase-lag errors resulted in a substantial loss in accuracy of the damping-in-roll results at subsonic velocities. The large number of calculations necessary in the reduction of the damping-in-roll data and the aileron rolling-moment data resulted in a small

decrease in accuracy of these results. The following table has been prepared to indicate the estimated probable percentage error of the rolling parameters through the velocity range:

Quantity	Subsonic (M = 0.69 to 0.85)	Transonic (M = 0.85 to 1.15)	Supersonic (M = 1.15 to 1.52)
C_{l_p}	±12	±10	±7
C_{l_δ}	±3	±5	±8

All hinge moments were measured with a possible error of $\pm 1\frac{1}{4}$ inch-pounds.

RESULTS AND DISCUSSION

Flight conditions existing at the time the data were obtained resulted in a Reynolds number variation with Mach number, as presented for reference in figure 6.

Hinge moments.- All hinge-moment data presented in this report were obtained during decelerated flight ($-3.5 \leq a_l \leq 0$) and at zero angle of attack.

The variation of hinge-moment coefficient with aileron deflection is presented in figure 7 over a Mach number range of 0.69 to 1.52. These coefficients were obtained for the aileron moving in both positive and negative directions, as is indicated by the curve symbols. The presented curves were faired through the average of the values obtained under the above two conditions since the reason for disagreement is not apparent at this time. At Mach numbers from 0.69 to 0.84 the variations are seen to be approximately linear, which indicates the center-of-pressure location of the lift load on the aileron to be invariant with deflection. The positive slopes of the curves indicate (for a trimmed condition) that the center of pressure was forward of the hinge line which was at 63.5 percent of the aileron root chord. At a Mach number of 0.91 the curve retains most of the positive slope, but, as Mach number is increased to 0.92, a large decrease in slope is observed. This decrease in slope is an indication of a rapid rearward shift in the center-of-pressure location, most probably the result of a loss in lift over the nose section of the aileron, and will be seen later in a different form. The variation of C_h with δ is also less linear at M = 0.92, indicating

a small rearward shift in center-of-pressure location with increasing deflections. The shapes of the hinge-moment-coefficient curves from $M = 0.95$ to $M = 1.52$ change only slightly, the curves decreasing in slope as Mach number is increased. At low aileron deflections the slopes of the curves remain positive, but at higher deflections the slope approaches zero and finally becomes negative at the highest deflections ($\pm 4^\circ$ to $\pm 5^\circ$), indicating the center of pressure has moved rearward with increasing deflection. Wind-tunnel-test results at $M = 1.9$ of a model similar to that used in the present investigation (reference 2) indicate that the center-of-pressure location at zero angle of attack was slightly behind the hinge line for the test deflection range of $\pm 10^\circ$. Differences in Mach number between the tunnel results and the present test results do not allow a valid comparison to be made.

It should be pointed out that the aileron was out of trim throughout the Mach range. This can be seen in figure 7 by the negative values of aileron hinge-moment coefficient at zero deflection. The variation of this out-of-trim moment with Mach number can be seen more easily in figure 8, which is a cross plot of figure 7 and presents the variation of hinge-moment coefficient with Mach number for various aileron deflections. The out-of-trim moment, indicated by the vertical displacement of the zero-deflection curve, was found to increase suddenly from a value of -0.005 at $M = 0.84$ to a maximum value of -0.011 at $M = 0.91$. The out-of-trim moment then decreased with increasing Mach number and approached a negligible value at $M = 1.52$. Out of trim has been previously experienced in "symmetrical" delta wings and is believed to be the result of small construction errors. Figure 8 again shows the large decrease in hinge-moment coefficients at $M = 0.91$. It should be pointed out, however, that the subsonic values, although large in comparison with the transonic and supersonic values, are actually small as compared with values obtained for other present-type ailerons.

Rolling parameters.- Figure 9 presents the damping-in-roll results of the investigation in coefficient form $\left(C_{l_p}\right)$ from $M = 0.69$ to $M = 1.52$. Included for comparison are theoretical C_{l_p} values (reference 3) for $1 \leq M \leq 1.6$ which are based on a 60° sweptback delta wing of identical plan form with no body. Also included for comparison is one wind-tunnel test point at $M = 1.62$ (reference 4) for a uniplanar-wing model with a ratio of wing span to body diameter approximately equal to that of this investigation. The shape of the damping curve obtained in this investigation is seen to compare favorably with linear theory within the comparable Mach range; the actual difference in magnitudes between the curves, however, cannot be explained by experimental inaccuracy. The ratio of wing damping with a body to wing damping without a body as obtained theoretically (reference 5) for an identical body-diameter - wing-span ratio as that tested indicates a 4-percent increase in C_{l_p}

for the body-on condition. It is therefore unlikely that disagreement in the comparison of test results with linear theory and the tunnel test point resulted primarily from body effects. It is believed that this disagreement is the result of mutual wing-interference effects of the cruciform configuration which were not considered in the uniplanar-wing theory. Subsonic values of C_{l_p} were found to be about 28 percent lower than predicted by lifting-line theory corrected for sweepback and compressibility effects (reference 6). At transonic velocities small abrupt changes occurred in C_{l_p} – its magnitude first increasing, then decreasing, and finally slightly increasing again with the total variation approximately 22 percent of the mean value.

The variation of aileron rolling-moment coefficient C_{l_δ} with Mach number is presented in figure 10 over a Mach range of 0.69 to 1.52. Calculations of C_{l_δ} based on linear theory (reference 7) are presented for comparison at supersonic Mach numbers. The test results were found to be from 15 percent to 30 percent lower than theory at supersonic Mach numbers. This difference is the result of the nonapplicable assumption of an infinitely thin airfoil utilized in the linear theory. Tunnel tests of a similar model (reference 8) have indicated no appreciable variation in C_{l_δ} with moderate changes in parting-line gap. It is interesting to note that there are no sharp breaks or rolling-moment losses at transonic Mach numbers. There was, however, a 45-percent decrease in C_{l_δ} between the Mach numbers of 1.0 and 1.5.

Figure 11 presents the variation of wing-tip helix angle per unit aileron deflection $\frac{pb/2V}{\delta}$ as calculated for a steady-state rolling condition from the C_{l_p} and C_{l_δ} data obtained in the present investigation. Introduced for comparison are rolling-effectiveness data obtained from free-flight rocket-test models (reference 1). The characteristic decrease in effectiveness at Mach numbers slightly less than $M = 1$ resulted primarily from the increased damping-in-roll values at these velocities, but this loss in effectiveness was small (10 percent) compared with other wing-aileron configurations, some of which have reversed effectiveness. The 60° wing-aileron combination tested also was found to retain 65 percent of the subsonic rolling-effectiveness value at $M = 1.5$.

CONCLUSIONS

The following conclusions may be drawn from the results of the investigation:

1. The half-delta tip aileron with a hinge-line location at 63.5 percent root chord, although slightly overbalanced throughout the flight, exhibited very small hinge-moment coefficients, especially at transonic and supersonic velocities. An abrupt reduction of hinge-moment coefficient occurred at a Mach number of 0.91, indicating a rapid rearward center-of-pressure shift.

2. The hinge-moment data indicate the aileron center of pressure to be constant with deflection at subsonic Mach numbers. At transonic and supersonic Mach numbers, however, a small rearward center-of-pressure shift was indicated for increasing positive and negative deflections.

3. It is believed that minor differences in the fabrication of "symmetrical" airfoil sections result in appreciable out-of-trim effects for airfoils which employ a large amount of aerodynamic balance.

4. At supersonic speeds the damping-in-roll coefficient C_{l_p} was found to be approximately 34 percent lower than predicted by linear theory within the comparable Mach range. At subsonic speeds C_{l_p} was found to be about 28 percent lower than corrected lifting-line theory. At transonic velocities small abrupt changes occurred in C_{l_p} – its magnitude first increasing, then decreasing, and finally slightly increasing again with the total variation approximately 22 percent of the mean value.

5. The aileron rolling-moment coefficient C_{l_δ} decreased 45 percent at Mach numbers from 1.0 to 1.5. There were no abrupt changes in C_{l_δ} in the transonic speed range.

6. The results indicate the rolling effectiveness (at small angles of attack) of a delta wing with tip ailerons to be very satisfactory at both subsonic and supersonic speeds. The characteristic loss in rolling

effectiveness at transonic speeds (found to be the result of increased damping in roll for the present configuration) was only 10 percent for the configuration tested, whereas other type wing–aileron combinations suffer serious reductions and even reversals in rolling effectiveness at these speeds.

Langley Aeronautical Laboratory
National Advisory Committee for Aeronautics
Langley Air Force Base, Va.

APPENDIX

METHOD OF REDUCING ROLL DATA

The following least-square application was utilized in determining the aileron rolling-moment-coefficient results from the telemeter data recorded in the investigation.

Symbols

L	total rolling moment measured at wing balance beam, ft-lb
L_{o_1}	out-of-trim rolling moment of damping wings, ft-lb
L_o	out-of-trim rolling moment of model, ft-lb
S_1	total wing area in both planes, 5.78 sq ft $\left[S_1 = (2S)\right]$
$C_{l_{p_1}}$	damping-in-roll coefficient, per radian $\left(\frac{\text{Total damping-in-roll moment}}{\frac{pb}{2V} qbS_1}\right)$
φ	angle of bank, radians
$\dot{\varphi},\ddot{\varphi}$	time derivatives of φ
I_x	moment of inertia of model about longitudinal axis, slug-ft^2
I_w	moment of inertia of damping wings about longitudinal axis of model, slug-ft^2
θ	angular deflection of damping wing under applied flight loads measured about model longitudinal axis, radians
$\dot{\theta},\ddot{\theta}$	time derivatives of θ
$t_1,t_2,t_3, \ldots$	time references

Method

The single-degree-of-freedom roll equation

$$I_x\ddot{\varphi} - C_{l_{p_1}} \frac{b}{2V} qbS_1\dot{\varphi} = -C_{l_\delta}\delta qbS + L_o \tag{1}$$

contains all the rolling moments applicable to the test model while in flight. The derivatives C_{l_δ} and $C_{l_{p_1}}$ are assumed to be constant at any particular Mach number. (This assumption was found to be valid within the accuracy of the present investigation.) For convenience, the following identities are substituted in the preceding equation:

$$\left.\begin{aligned} K_1 &= -C_{l_{p_1}} \frac{b}{2V} qbS_1 \\ K_2 &= -C_{l_\delta} qbS \\ K_3 &= L_o \end{aligned}\right\} \tag{2}$$

The resulting equation

$$I_x\ddot{\varphi} + K_1\dot{\varphi} = K_2\delta + K_3$$

is multiplied by each of its variables to obtain:

$$I_x\ddot{\varphi}^2 + K_1\dot{\varphi}\ddot{\varphi} = K_2\delta\ddot{\varphi} + K_3\ddot{\varphi} \tag{3a}$$

$$I_x\ddot{\varphi}\dot{\varphi} + K_1\dot{\varphi}^2 = K_2\delta\dot{\varphi} + K_3\dot{\varphi} \tag{3b}$$

$$I_x\ddot{\varphi}\delta + K_1\dot{\varphi}\delta = K_2\delta^2 + K_3\delta \tag{3c}$$

By recording several simultaneous measurements of the three variables ($\ddot{\varphi}$, $\dot{\varphi}$, and δ) at constant Mach number from the telemeter record, the following constants can be evaluated:

$$A = \sum(\ddot{\varphi}^2) = \ddot{\varphi}_{t_1}{}^2 + \ddot{\varphi}_{t_2}{}^2 + \ddot{\varphi}_{t_3}{}^2 + \cdots$$

$$B = \sum(\ddot{\varphi}\dot{\varphi}) = \ddot{\varphi}_{t_1}\dot{\varphi}_{t_1} + \ddot{\varphi}_{t_2}\dot{\varphi}_{t_2} + \ddot{\varphi}_{t_3}\dot{\varphi}_{t_3} + \cdots$$

$$C = \sum(\ddot{\varphi}\delta) = \ddot{\varphi}_{t_1}\delta_{t_1} + \ddot{\varphi}_{t_2}\delta_{t_2} + \ddot{\varphi}_{t_3}\delta_{t_3} + \cdots$$

$$\left.\begin{aligned} E &= \sum(\ddot{\varphi}) \\ F &= \sum(\dot{\varphi}^2) \\ G &= \sum(\delta\dot{\varphi}) \\ H &= \sum(\dot{\varphi}) \\ J &= \sum(\delta^2) \\ L &= \sum(\delta) \end{aligned}\right\} \text{Evaluated as A, B, and C}$$

Replacing the variables in equations (3) with the above measured constants yields three simultaneous equations

$$I_x A + K_1 B = K_2 C + K_3 E \tag{4a}$$

$$I_x B + K_1 F = K_2 G + K_3 H \tag{4b}$$

$$I_x C + K_1 G = K_2 J + K_3 L \tag{4c}$$

The three unknowns K_1, K_2, and K_3 are obtained from the solution of these equations, and, from equation (2), C_{l_δ} is calculated.

Rather than use the model rolling response to determine wing damping in roll, a more accurate means was used in which the actual rolling

moment of the wings was measured through the use of a rolling-moment balance. This balance measured the total moment on the wings which included the moment due to wing inertia, wing damping moment, and out-of-trim rolling moment. The following equation contains all the component moments measured by the balance:

$$L = I_w(\ddot{\varphi} - \ddot{\theta}) - C_{l_p} \frac{b}{2V} qbS(\dot{\varphi} - \dot{\theta}) + L_{o_l}$$

The least-square application to this equation was used as before to determine the damping-in-roll coefficient C_{l_p}.

The variables used in the least-square applications were obtained from the telemeter record, a sample of which is illustrated in figure 12.

REFERENCES

1. Sandahl, Carl A., and Strass, H. Kurt: Comparative Tests of the Rolling Effectiveness of Constant-Chord, Full-Delta, and Half-Delta Ailerons on Delta Wings at Transonic and Supersonic Speeds. NACA RM L9J26, 1949.

2. Conner, D. William, and May, Ellery B., Jr.: Control Effectiveness Load and Hinge-Moment Characteristics of a Tip Control Surface on a Delta Wing at a Mach Number of 1.9. NACA RM L9H05, 1949.

3. Brown, Clinton E., and Adams, Mac C.: Damping in Pitch and Roll of Triangular Wings at Supersonic Speeds. NACA Rep. 892, 1948.

4. Brown, Clinton E., and Heinke, Harry S., Jr.: Preliminary Wind-Tunnel Tests of Triangular and Rectangular Wings in Steady Roll at Mach Numbers of 1.62 and 1.92. NACA RM L8L30, 1949.

5. Lomax, Harvard, and Heaslet, Max. A.: Damping-in-Roll Calculations for Slender Swept-Back Wings and Slender Wing-Body Combinations. NACA TN 1950, 1949.

6. Polhamus, Edward C.: A Simple Method of Estimating the Subsonic Lift and Damping in Roll of Sweptback Wings. NACA TN 1862, 1949.

7. Lagerstrom, P. A., and Graham, Martha E.: Linearized Theory of Supersonic Control Surfaces. Jour. Aero. Sci., vol. 16, no. 1, Jan. 1949, pp. 31-34.

8. Conner, D. William, and May, Ellery B., Jr.: Control Effectiveness and Hinge-Moment Characteristics of a Tip Control Surface on a Low-Aspect-Ratio Pointed Wing at a Mach Number of 1.9. NACA RM L9H26, 1949.

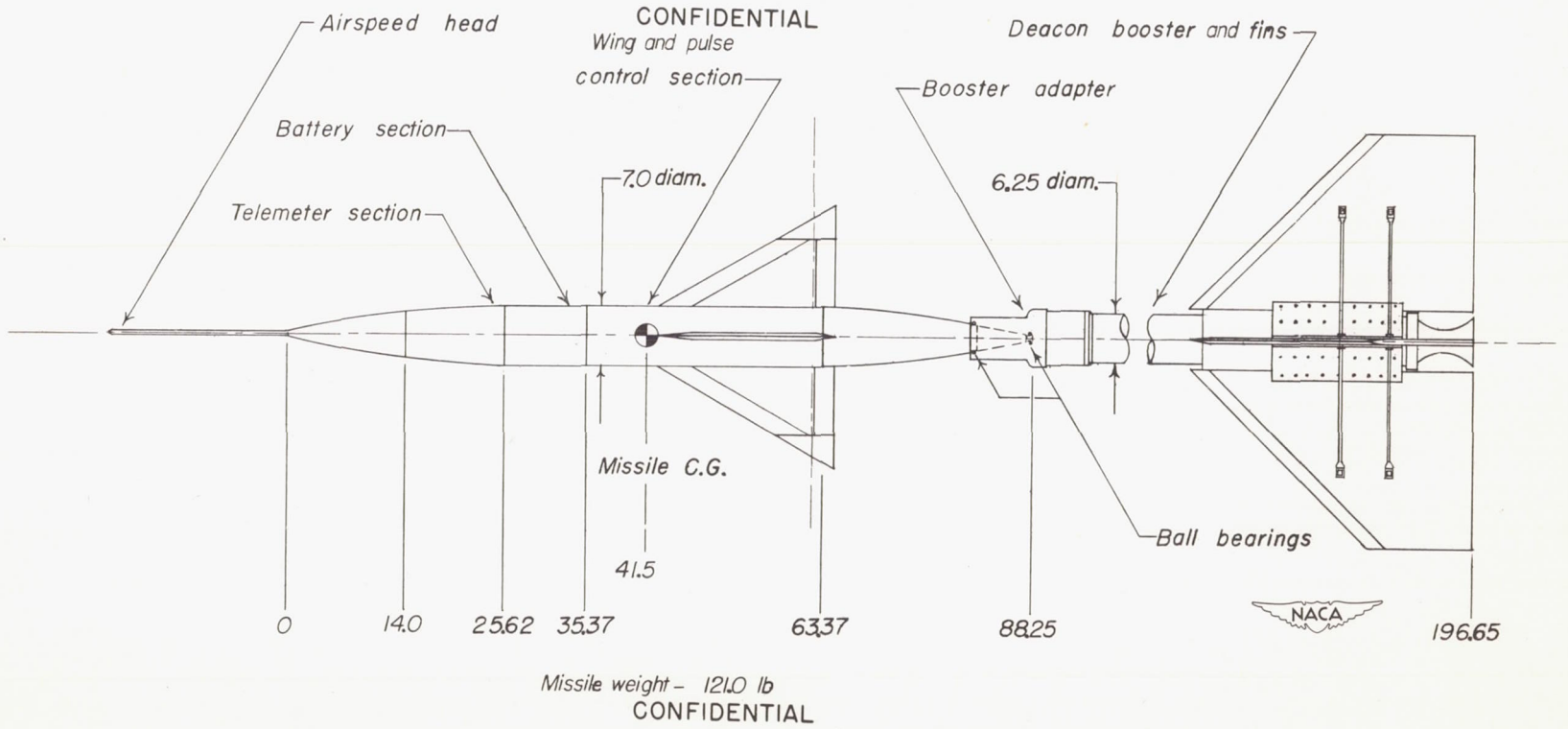

Figure 1.- General arrangement of the pulsed-control roll research vehicle and booster; all dimensions in inches.

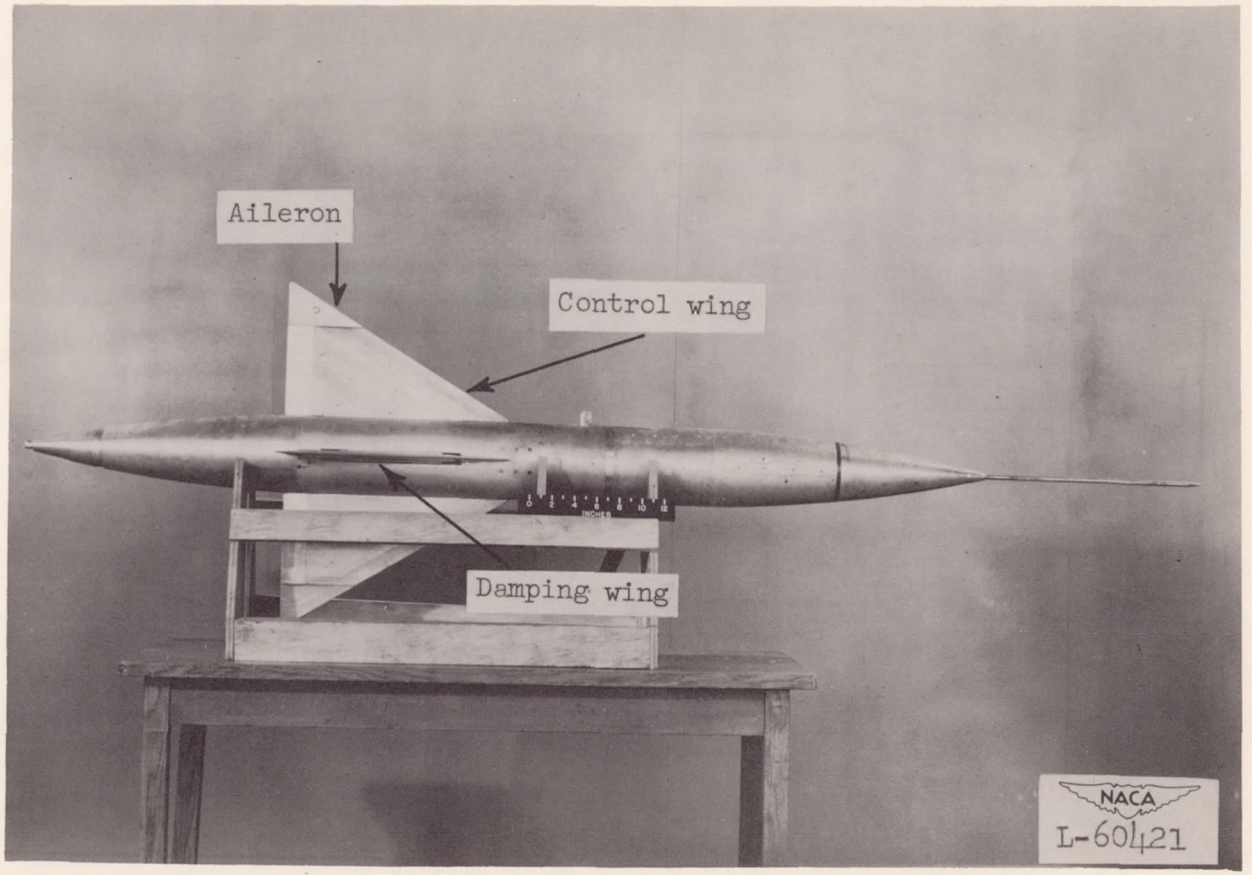

Figure 2.- Photograph of pulsed-control roll research vehicle.

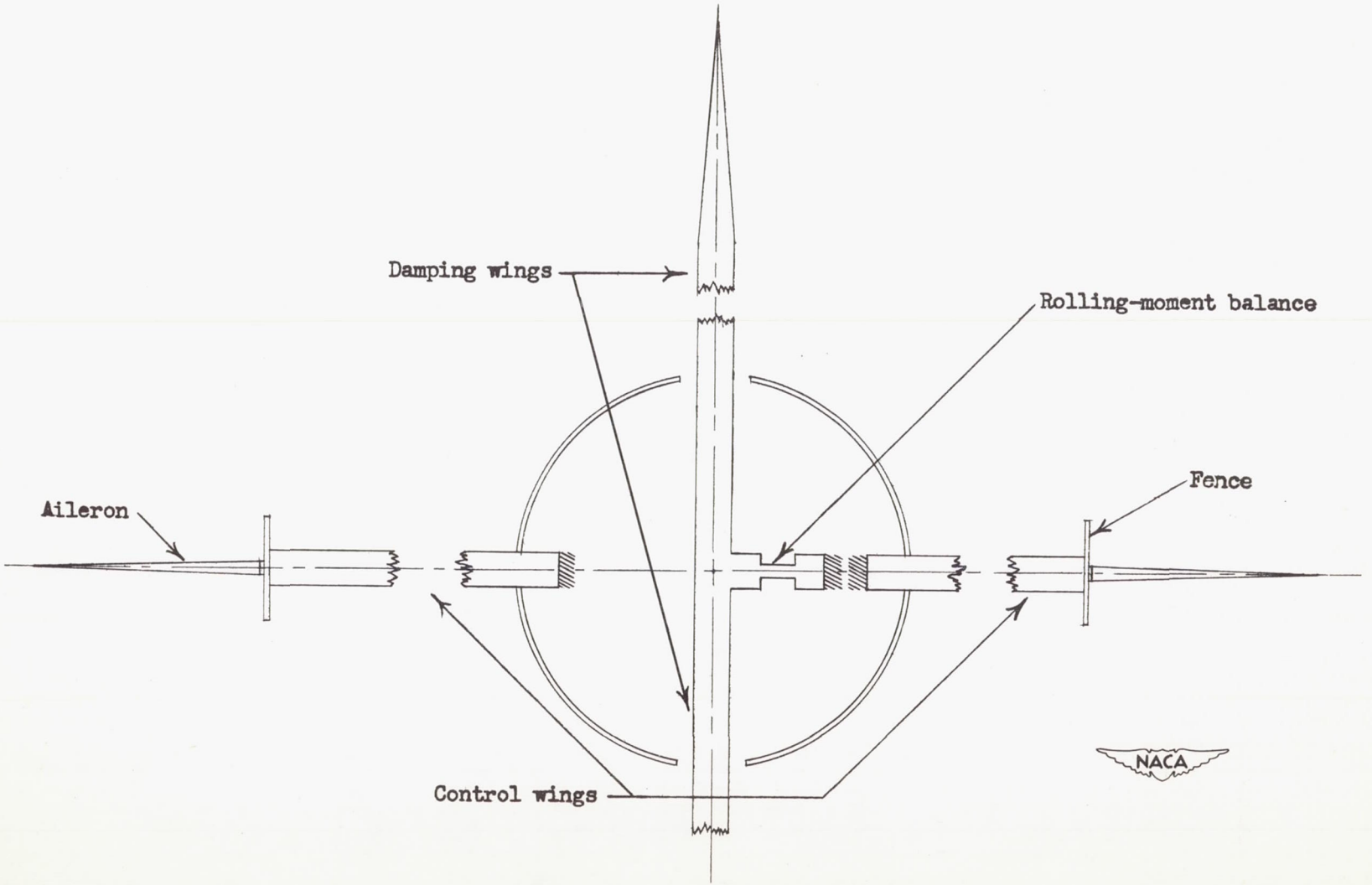

Figure 3.– Schematic diagram of wing balance system.

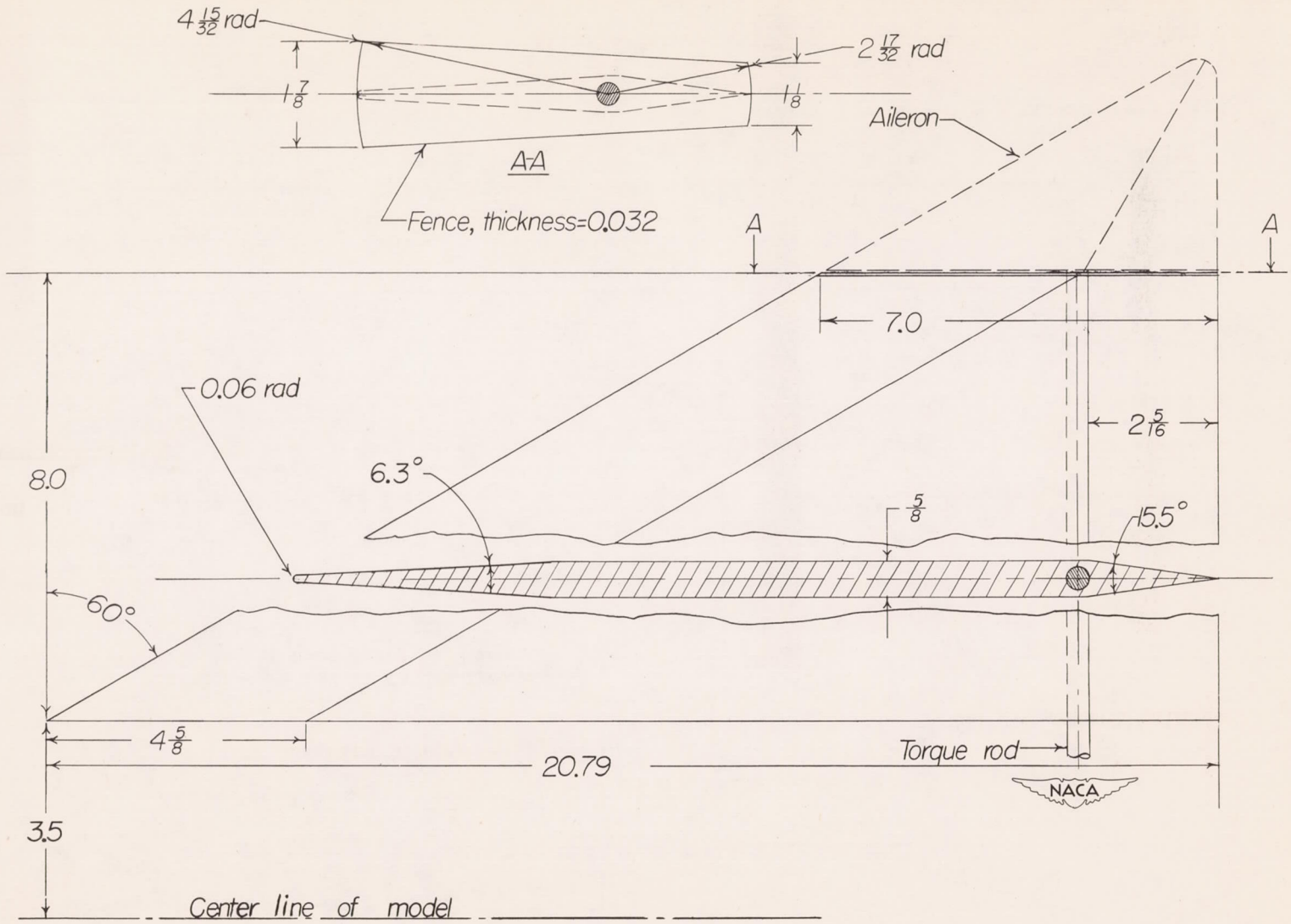

(a) Details of wing and fence.

Figure 4.- Control wing; all dimensions in inches.

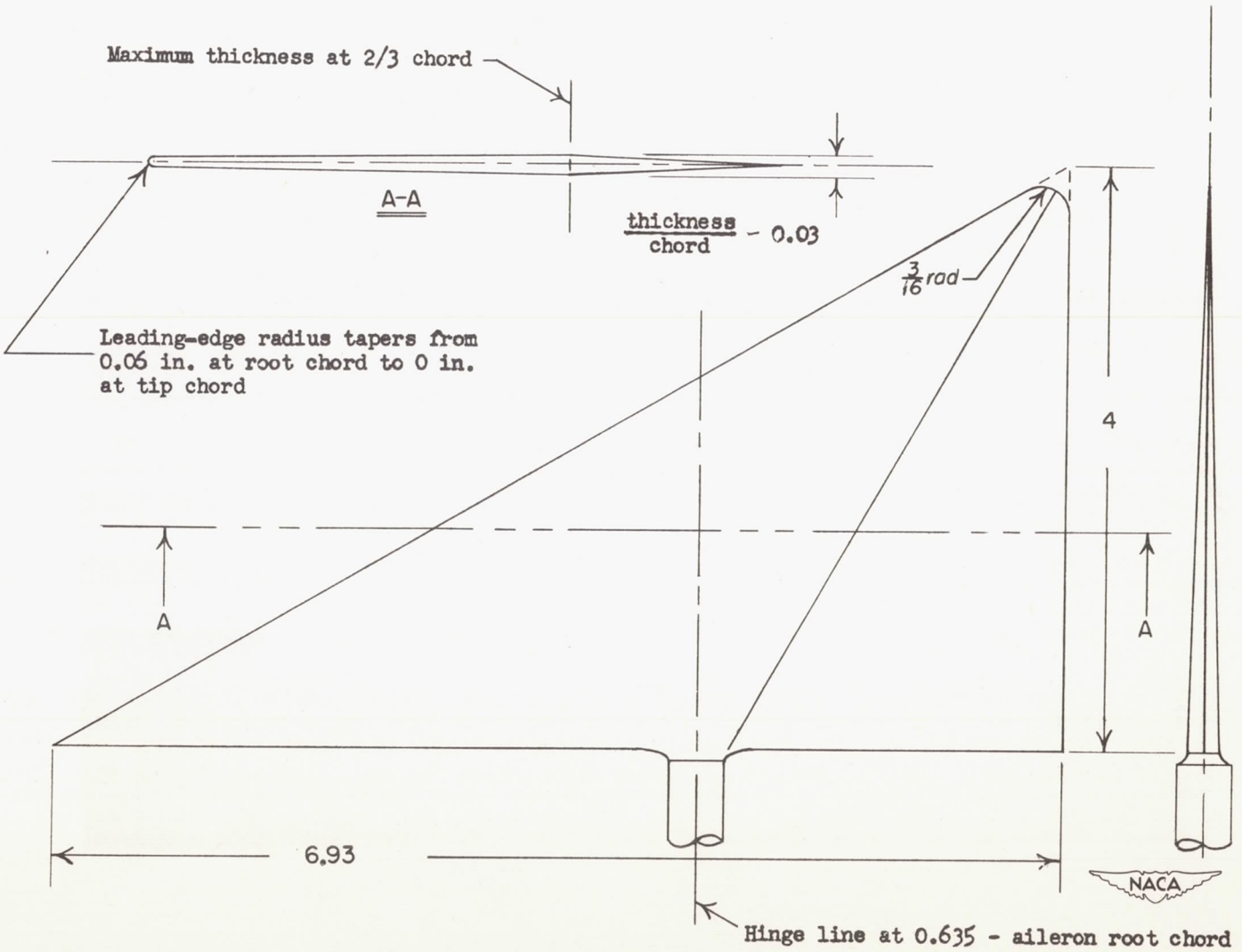

(b) Details of aileron.

Figure 4.- Concluded.

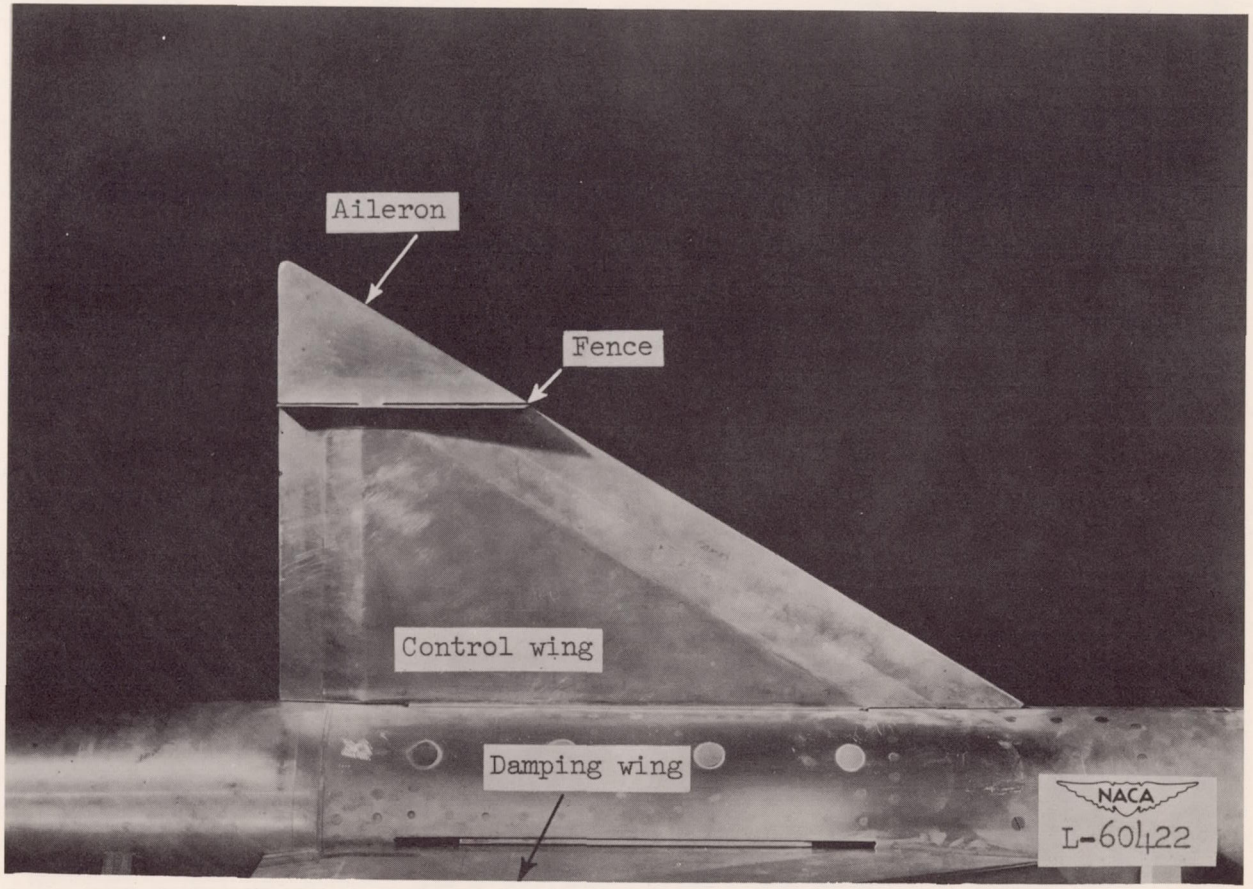

Figure 5.- Photograph of wing and aileron.

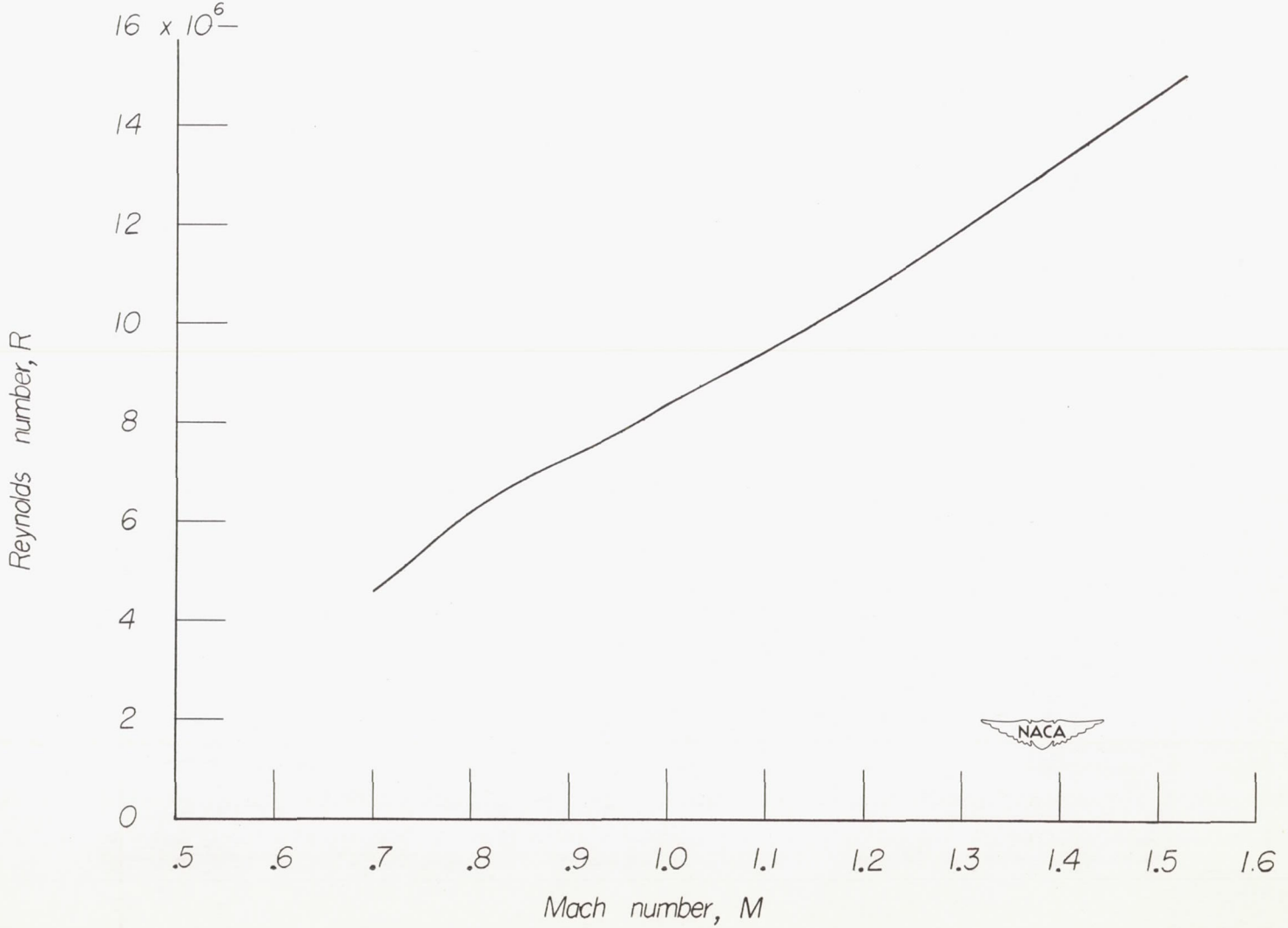

Figure 6.- Variation of free-flight Reynolds number with Mach number.

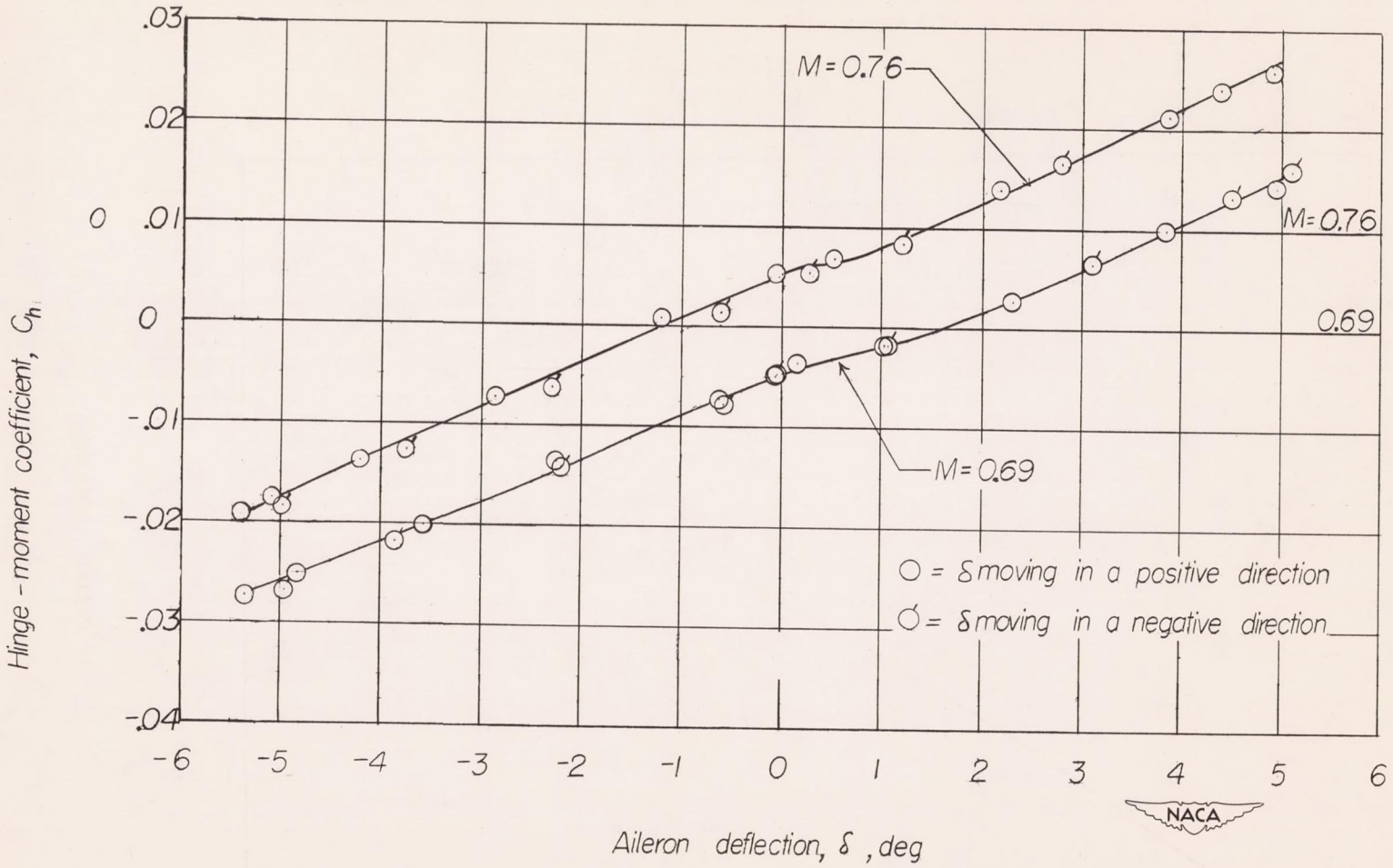

Figure 7.- Variation of aileron hinge-moment coefficient with aileron deflection for M = 0.69 to M = 1.52 at zero angle of attack.

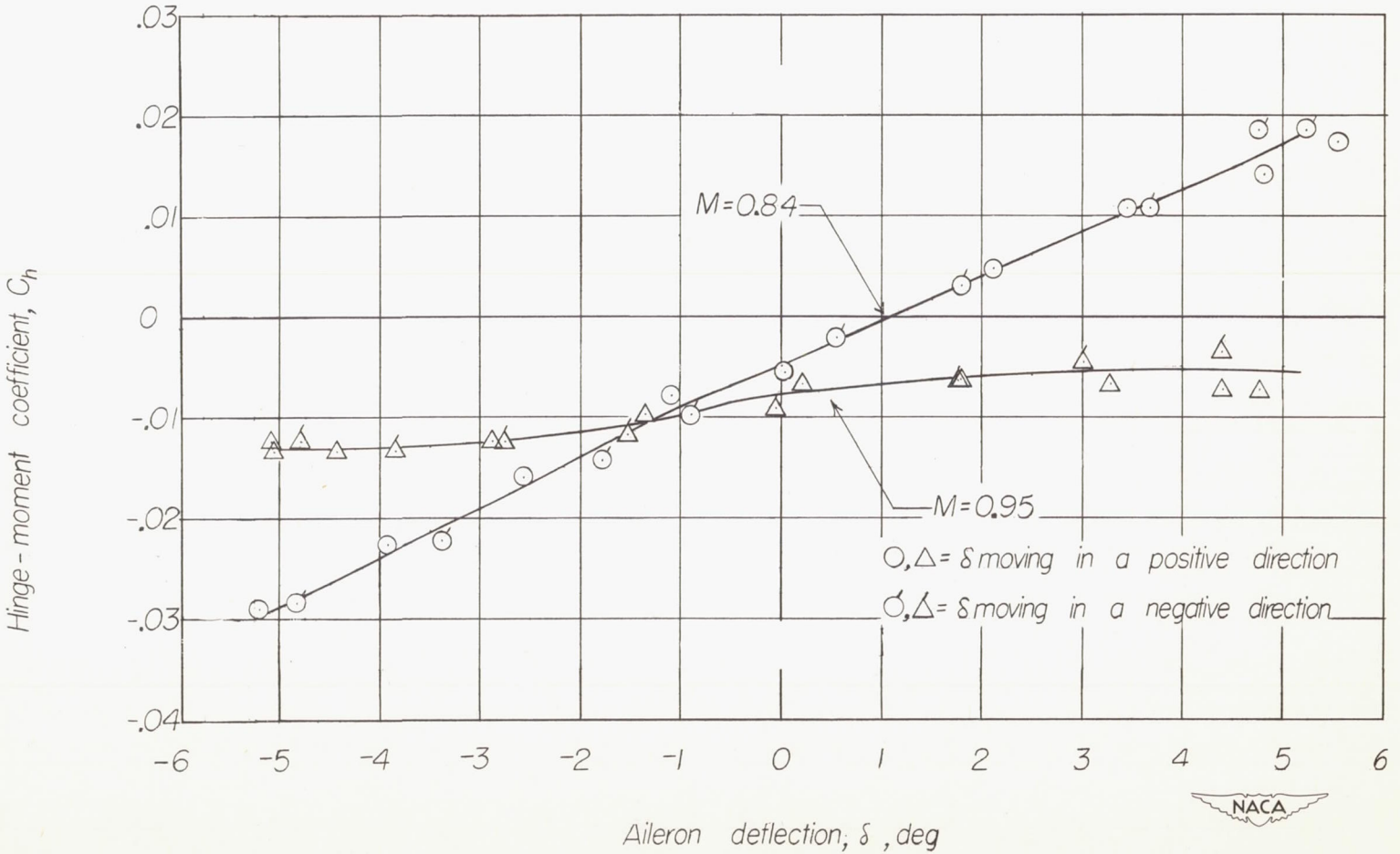

Figure 7.- Continued.

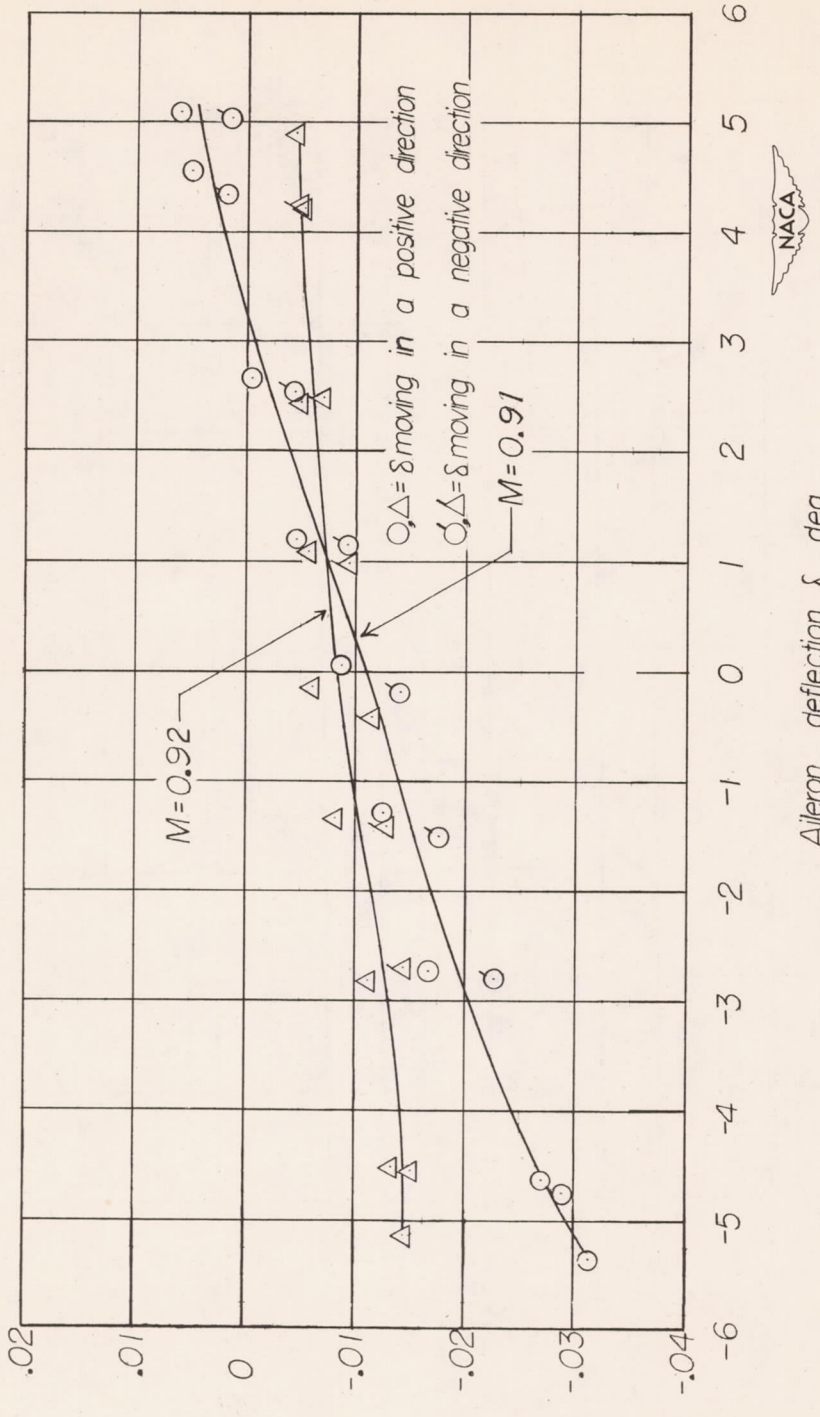

Figure 7.- Continued.

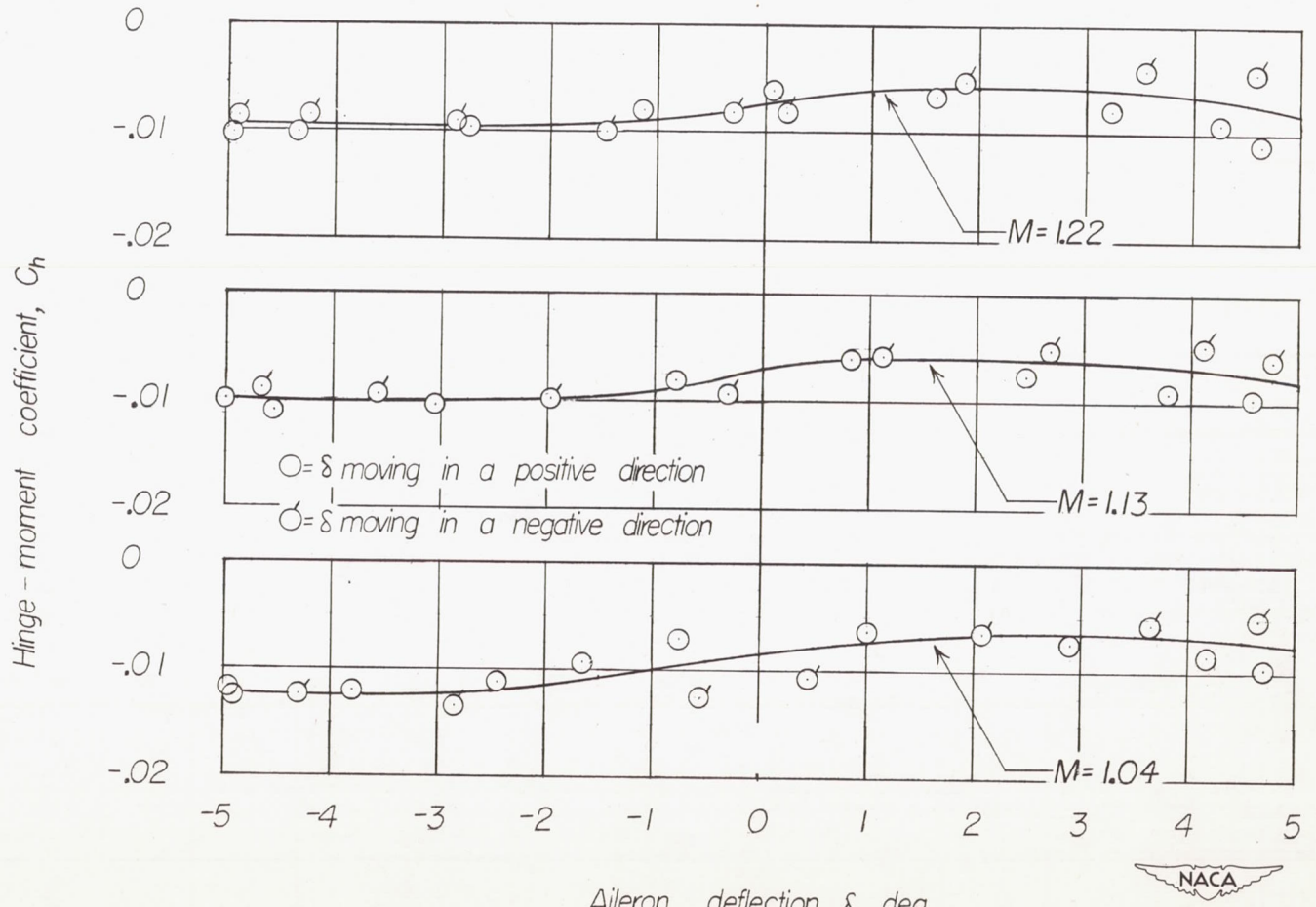

Figure 7.- Continued.

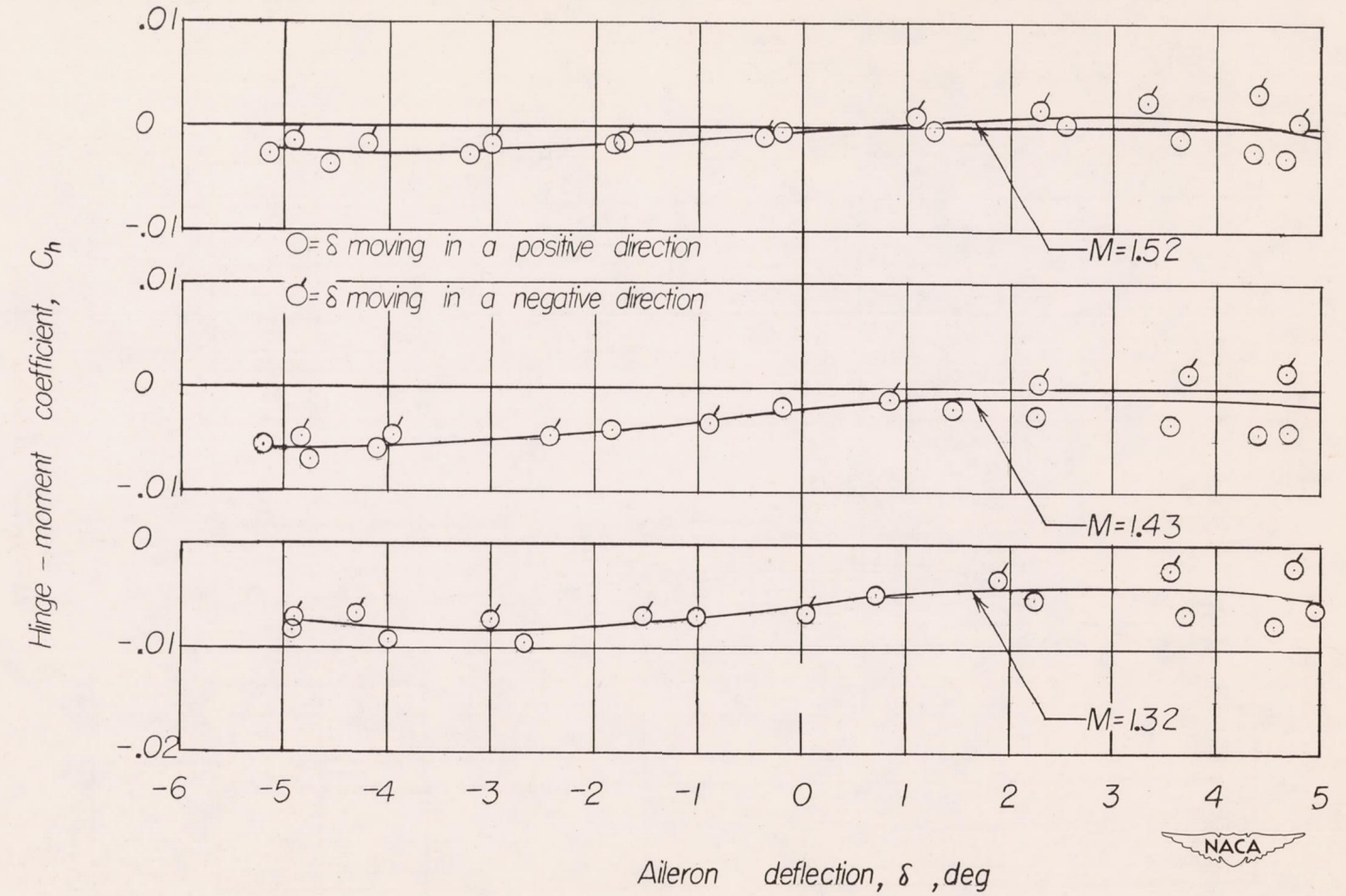

Figure 7.- Concluded.

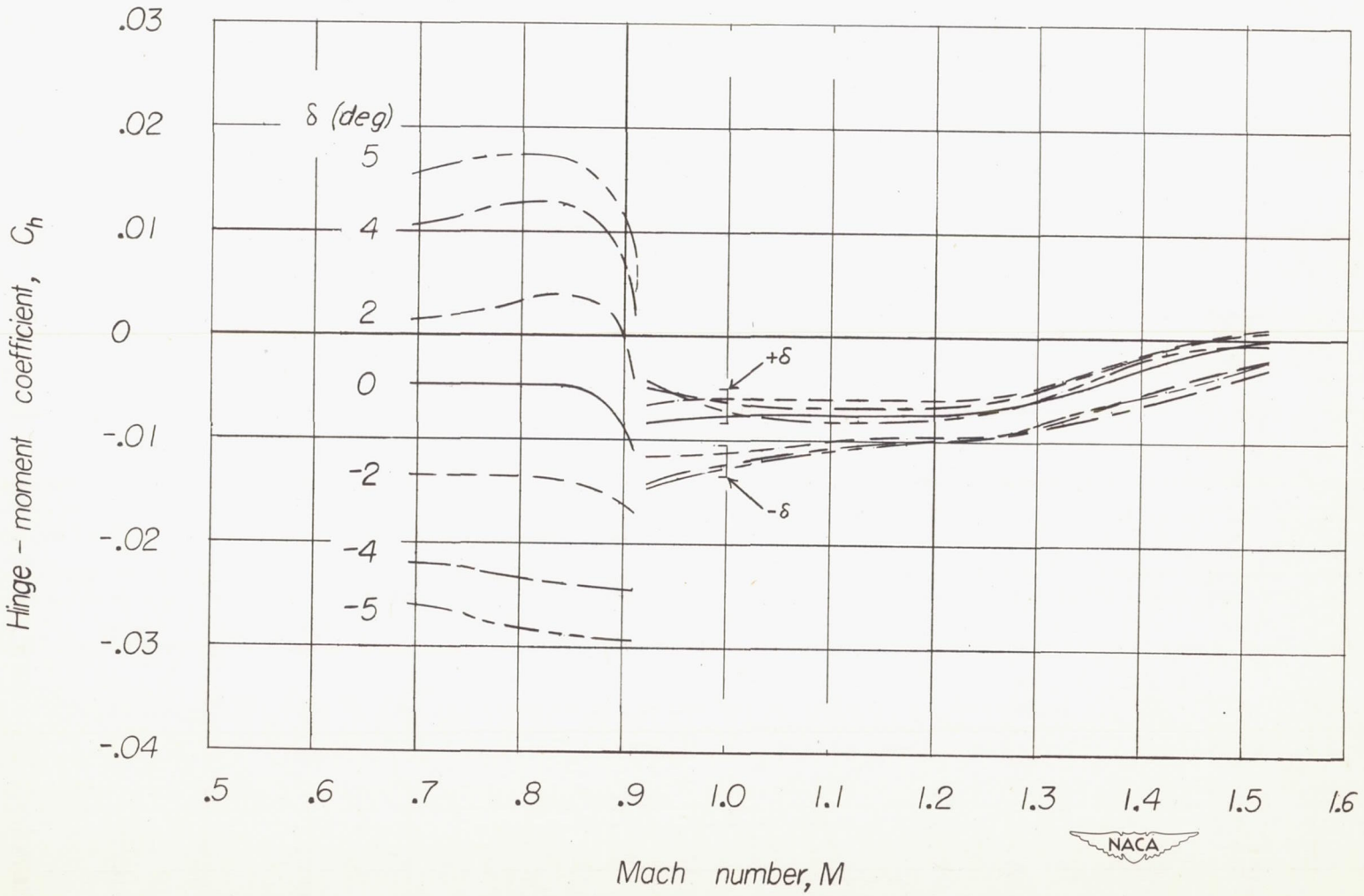

Figure 8.- Aileron hinge-moment coefficient against Mach number for various aileron deflections with zero angle of attack.

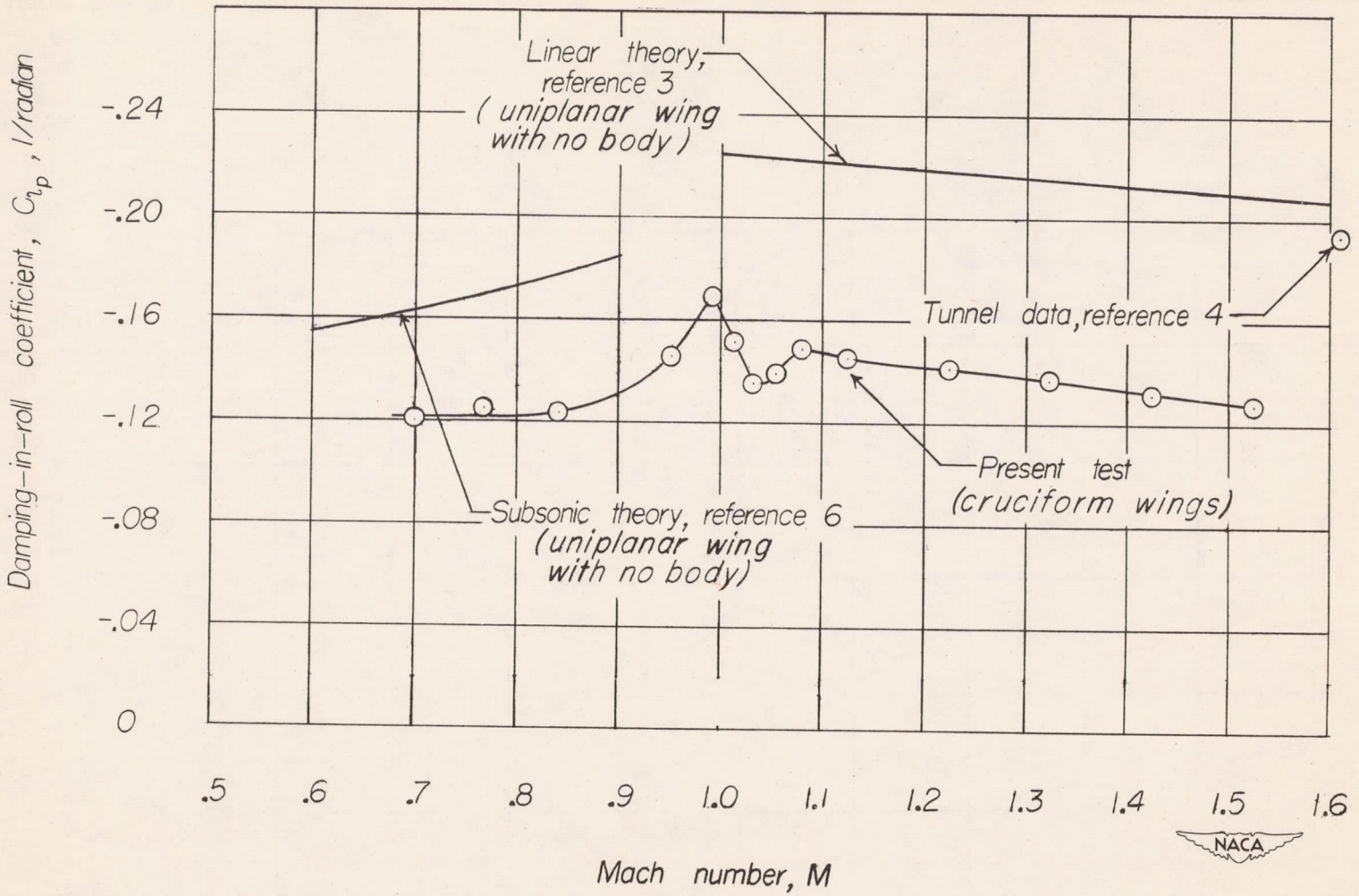

Figure 9.- Damping-in-roll-coefficient variation with Mach number as computed from experimental data.

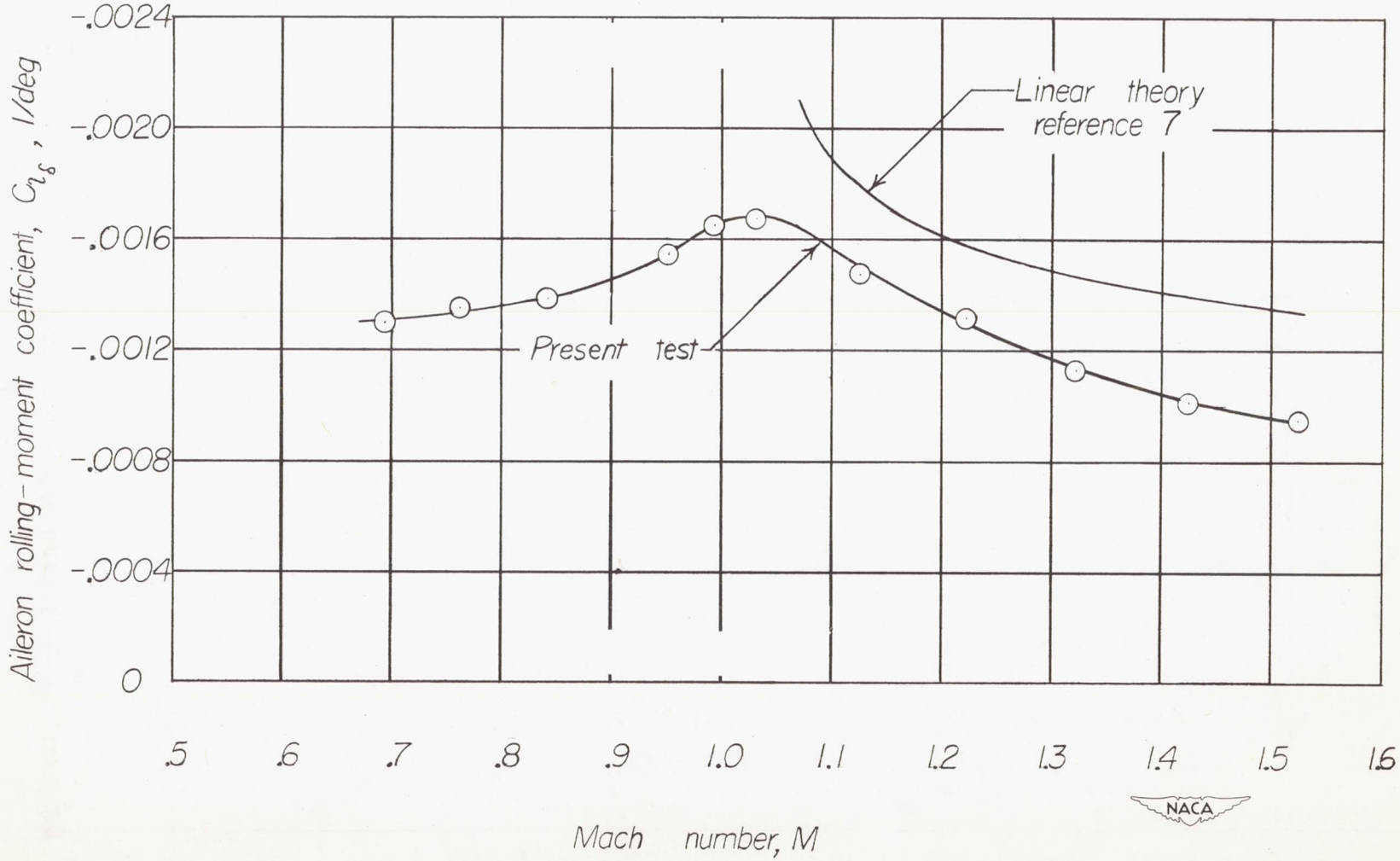

Figure 10.- Variation of aileron rolling-moment coefficient with Mach number as computed from experimental data.

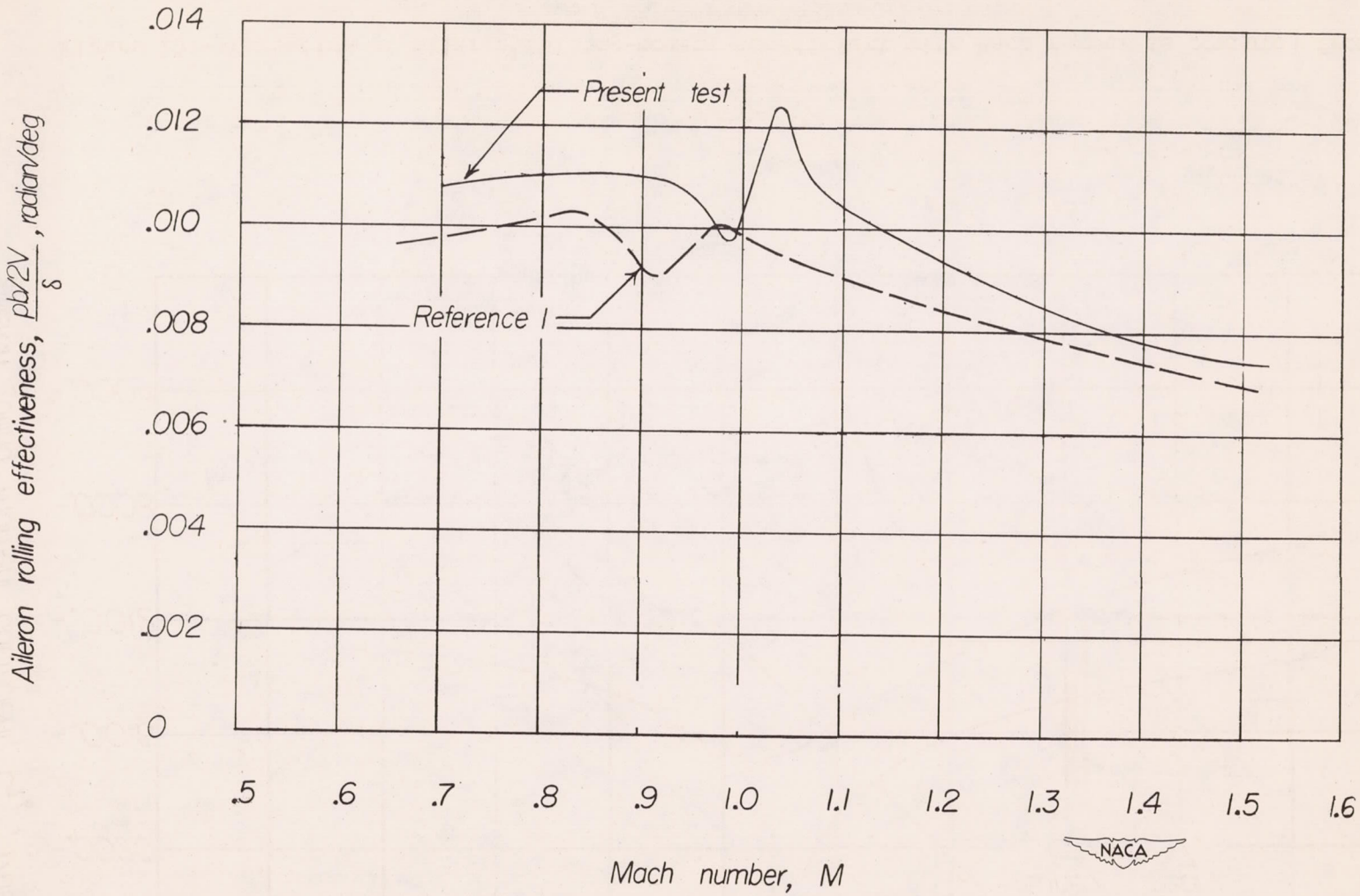

Figure 11.- Comparison of previous free-flight rocket-test results with results calculated from data obtained in present investigation.

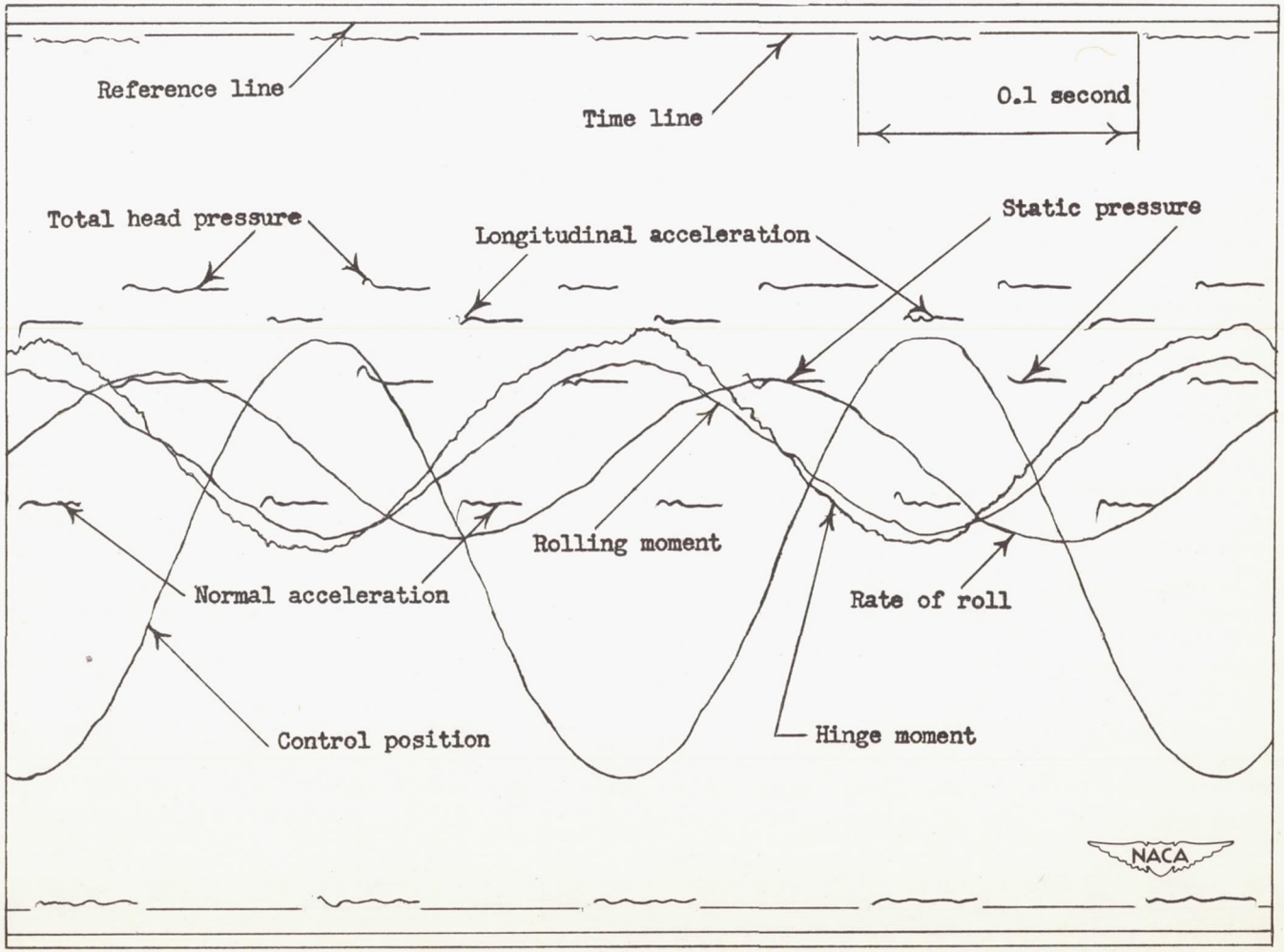

Figure 12.- Sample telemeter record.